

Observing ENSO Reversals using RegCM4 and Satellite Data in the Philippines during the Southwest Monsoon Season

Raymund T. Masangya

Technological University of the Philippines

Abstract

Introduction: Investigations into the temporal shifts and heightened intensity of the southwest monsoon (SWM) are of equal importance to the Philippines based to the fundamental impact of the SWM on the country's precipitation patterns. As a principal determinant of the rainfall climatology, the SWM significantly influences the distribution and availability of water resources, which are indispensable for various sectors including agriculture, industry, and commerce. Given that the SWM serves as a primary source of water supply in the Philippines, elucidating its alterations is imperative for informed decision-making and adaptive measures to address potential challenges posed by changing climatic conditions. Moreover, such research endeavors contribute to enhancing resilience and sustainability across key sectors, facilitating effective resource management strategies and fostering socio-economic development in the region.

Objectives: This research investigated whether the behavior of the possible indicators (precipitation, wind, sea level pressure and sea surface temperature) can be captured by a regional climate model (RegCM4).

Methods: The methodology employed in this study involved the analysis of various indicators to assess changes in rainfall patterns, particularly focusing on the southwest monsoon (SWM) season in the Philippines. Four key indicators—wind, sea surface temperature (SST), sea level pressure, and large-scale precipitation—were scrutinized using data sets from multiple sources. Specifically, wind, SST, and sea level pressure data were obtained from the ECMWF ERA-Interim reanalysis data set spanning from 1979 to the present. This data set provided comprehensive coverage with 60 vertical levels and a spatial resolution of 0.75° latitude x 0.75° longitude. Additionally, SST data from the NOAA Optimum Interpolation SST version 2 (V2) and mean sea level pressure data from the NCEP/NCAR Reanalysis data set were utilized. Furthermore, the study incorporated large-scale precipitation data from the TRMM data set to assess rainfall behavior over a broader spatial context. Moreover, the methodology employed a combination of observational data analysis and numerical modelling to comprehensively investigate changes in SWM rainfall patterns and associated atmospheric dynamics in the Philippines.

Results: Results showed that the model captured the general characteristics of the observed indicators (sea level pressure and SST), especially during EN and LN events but fails to adequately represent the corresponding effect on precipitation. In addition to this, the inability of the model to capture the wind patterns result into failure in capturing the behavior of precipitation. The results showed that the underestimation (overestimation) of winds made the precipitation becomes drier (wetter) in condition and these findings needs a future study.

Conclusions: The conclusion of the study indicates that while the numerical experiment successfully replicates certain observed data patterns, such as the precipitation anomaly during El Niño (EN) events, discrepancies exist, particularly in capturing anomalies in the western part of the country during normal years and wind patterns. Despite these shortcomings, the model aligns well with observed behaviors of sea surface temperature (SST) and sea level pressure during the ENSO signal reversal. Overall, the findings underscore the significance of SST, wind, and pressure as indicators linked to rainfall behavior in the western regions of the Philippines during the southwest monsoon (SWM) season.

Keywords: ENSO, Satellite Data, Southwest Monsoon, RegCM4

1. Introduction

Rainfall events are mainly affected by synoptic systems such as monsoons, El Niño Southern Oscillation (ENSO), and mesoscale systems (de las

Alas and Buan, 1986; Francisco et al., 2006; Jose et al., 1996). In the Philippines, precipitation is greatly influenced by the Southwest Monsoon (SWM). Based on Asuncion and Jose (1980), 43% of mean

annual rainfall in the Philippines comes from the SWM, which is observed during the boreal summer (July to August). Rainfall in the western region of the country is most affected during this season. The SWM came from the Indian Ocean Anticyclones, which had a characteristics of warm, humid and regions where convective activity forms. From the anticyclone in the Indian Ocean it generally reaches our country (mostly at the western region) as a south-westerly stream. Observed data from meteorological stations show variations on the onset of the SWM with topography and elevation. Note that the SWM is detected by stations located at the western part of the country, which is of Climate type I. This climate type were located at the Western regions of Luzon, Mindoro, Negros, and Palawan. This region experienced two pronounced seasons, wherein the wet season from May to October and the rest is the dry season. The SWM can start as early as April but generally develops in May, peaks in August, and ends in October. However, there can be a tendency for the season to extend up to December (Flores and Balagot, 1969). The condition of SST is very important in the mechanism of the hydrological cycle in the tropics. Meehl et al. (1994) study the connection of land-sea thermal contrasts to the Asian summer monsoon. They found out that the strength of the summer monsoons are associated with the temperature difference of land-sea interactions. Stronger summer monsoons has a larger land-sea thermal contrasts. Also, according to Roxy et al. (2012), there is a spatial variability in the Asian Monsoon Region in the local intra-seasonal SST-precipitation relationship. According to Xie et al. (2009), the SST and precipitation relationship has a direct effect to each other, wherein local maxima (minima) SST warming results to enhanced (reduced) precipitation in the tropics. However, rainfall-SST relationship is not simply a cause and effect mechanism. According to Wu et al. (2010), there is an asymmetry of SST in the WNP, wherein there is a cold SST anomaly (SSTA) during El Niño and warm SSTA during La Niña. Lyon and Camargo (2008) state that the asymmetry between the SST during EN and LN is due to the remote forcing. Wu (2009) classified the entire 27 summers into ENSO-developing (DV), ENSO-decaying (DC) and remaining years (RM) from 1971 – 2000 period.

Winds have also some noticeable characteristics during ENSO and some studies found the asymmetry during EN and LN years. During EN and LN, the wind speed anomalies are dominant in the transitional zone between monsoon westerly and trade easterly and this is caused by the asymmetry of the latent heat flux anomalies, which can cause also the change in precipitation (Wu et al., 2010). The low level westerly (easterly) winds is associated with the formation of anomalous cyclonic (anticyclonic) circulation during JAS of EN (LN), which can cause an increase (decrease) of moisture in the Philippines (Lyon and Camargo, 2009). The change in SLP during ENSO also plays a very important role in changing the rainfall in the country. Based on the analysis of Yu et al. (2010), the first SLP mode is associated with the variability of the Aleutian low and there can be an asymmetry during EN and LN phase. He concluded that the EN (LN) enhances (weakens) the Aleutian low which has a negative (positive) SLP anomalies. Roy et al. (2010) also have the same results and he linked this to a higher solar activity in the North Pacific, which can cause a weakening of the Aleutian low. The asymmetry of pressure during ENSO phase in boreal summer can cause rainfall anomalies of opposite signs to develop in the North Central Philippines. This indicates an increase (decrease) in precipitation during EN (LN) phase with the asymmetry of pressure and this is the reason for choosing pressure as one of the possible factors in the decline of rainfall during SWM season..

2. Objectives

The objective of this research is to examine the ability of the model to capture the patterns of the observed indicators that affect SWM rainfall. Results can provide useful information for future studies which intend to use the model for studying the SWM rainfall.

3. Methods

3.1 Data Sets Used

In this study, four possible indicators of the change in rainfall are analyzed: wind, sea surface temperature (SST), sea level pressure, and large-scale precipitation. Wind, SST and sea level pressure data is obtained from the ECMWF ERA-Interim reanalysis data set from 1979 to present, which was produced with a 2006 version of the Integrated Forecast Model (IFS Cy31r2). ERA-

Interim superseded the ERA-40 as a new version of the extended reanalysis. The ERA-Interim data set has 60 vertical levels from the surface up to 0.1 hPa. This study will use monthly surface winds from 1998 to 2014 and the spatial resolution of this data is 0.75° latitude x 0.75° longitude global grid (see <http://apps.ecmwf.int/datasets/data/interim-full-moda/levtype=sfc/>, last accessed October 2014). According to Dee et al. (2011), ERA-Interim improves the hydrological cycle that results in improving the precipitation and other variables compare to ERA 40.

For comparison in the ERA Interim data, this study used some other reanalysis data that can help in evaluating the behavior of the possible indicators. Another SST data was taken from the NOAA Optimum Interpolation (OI) SST version 2 (V2) from 1998 to 2014 during the southwest monsoon season. The spatial resolution of this data is 1.0° latitude x 1.0° longitude global grid (180x360), which covers an area from 89.5°N – 89.5°S and 0.5°E – 359.5°E. According to Stock et al. (2015), NOAA OISST version 2 agrees the data in situ measurements particularly in the large marine ecosystem in the U.S.. We used another mean sea level pressure (mslp) from NCEP/NCAR Reanalysis data set. This 2.5° resolution data has a temporal coverage from 1948 up to present but this study will just use the monthly data from 1998 to 2014 (see <http://www.esrl.noaa.gov/psd/data/gridded/data.ncep.reanalysis.derived.surface.html>, last accessed October 2014) . Finally, the large-scale precipitation was also investigated in this study. The TRMM data set is widely used for validation of rainfall in terms of large-scale system as well as in local scale (e.g. Lang et al., 2007; Franchito et al., 2009). Observed rainfall data during the southwest monsoon season was analyzed with large-scale precipitation and check if the behavior was the same in the large area. The inclusion of large-scale precipitation was to have a context of the station data in terms of a spatial maps.

3.2 Classification of ENSO Years

El Niño (EN) and La Niña (LN) events were classified using the SST anomalies in the tropical Pacific basin, which is commonly called the Niño 3.4 region (5°S – 5°N and 120° – 170° W). The threshold value of EN (LN) event is declared at least 0.5 °C (-0.5 °C) over a

period of three consecutive months of ERSST.v4 SST anomalies for warm (cold) episode. (e.g. Trenberth 1997; Moya and Malayang 2004; Kao and Yu 2009). We used the same methodology as that of Cruz et al. (2013) and Lyon and Camargo (2009) in classifying the El Niño and La Niña years. The warm or cold episode should last for six or more consecutive overlapping seasons and this episode must start from June to August. Hence, 2007 and 2011 is not included in the LN years because it starts in July. The baseline period (1971-2000) was derived from the Climate Prediction Center of the National Weather Service (see http://www.cpc.noaa.gov/products/analysis_monitoring/ensostuff/ensoyears.shtml, last accessed October 2015). Table 1 and Table 2 show the list of El Niño and La Niña years from 1998 to 2014.

Table 1. List of the Oceanic Niño Index (ONI) (3-month running mean of ERSST.v4 SST anomalies in the Niño 3.4 region).

Year	AMJ	MJJ	JJA	JAS	ASO	SON
1998	0.5	-0.1	-0.7	-1	-1.2	-1.2
1999	-0.9	-1	-1	-1	-1.1	-1.2
2000	-0.7	-0.7	-0.6	-0.5	-0.6	-0.7
2001	-0.2	-0.1	0	-0.1	-0.1	-0.2
2002	0.4	0.7	0.8	0.9	1	1.2
2003	-0.2	-0.1	0.1	0.2	0.3	0.4
2004	0.2	0.3	0.5	0.7	0.7	0.7
2005	0.4	0.2	0.1	0	0	-0.1
2006	0	0.1	0.2	0.3	0.5	0.8
2007	-0.2	-0.2	-0.3	-0.6	-0.8	-1.1
2008	-0.7	-0.5	-0.3	-0.2	-0.2	-0.3
2009	0.2	0.4	0.5	0.6	0.7	1
2010	0	-0.4	-0.8	-1.1	-1.3	-1.4
2011	-0.3	-0.2	-0.3	-0.5	-0.7	-0.9
2012	-0.3	-0.1	0.1	0.3	0.4	0.4
2013	-0.2	-0.2	-0.2	-0.2	-0.2	-0.2
2014	0	0	0	0	0.2	0.4

Table 2. List of Classification of Years from 1998 to 2014 for Normal, La Niña and El Niño Years.

	Year
Normal Years	2001, 2003, 2005, 2006, 2007, 2008, 2011, 2012, 2013, 2014
La Niña	1998, 1999, 2000, 2010
El Niño	2002, 2004, 2009

3.3 Philippines ENSO Signal Reversal and the Regional Atmospheric Circulation

The signal reversal was fully investigated by [Lyon et al. \(2006\)](#) and [Lyon and Camargo \(2009\)](#). They used composite in order to see the difference between EN and LN years. This method was adapted, which investigates the reversal of the atmospheric circulation during EN and LN years in the Philippines. In [Lyon and Camargo \(2009\)](#), the significance of their results was based on the below and above average in 90% and 95% confidence level. Also, [Lyon et al. \(2006\)](#) used below and above median in their analyses and the statistical significance was 90% and 95% confidence level. However, both of the studies covered the period from 1950 to 2002 and this method was performed in this study in order to have a comparison of the results and also to look for similar patterns from the study of [Lyon and Camargo \(2009\)](#). In this study we will call it as an “ENSO signal reversal”, because this study focuses on the ENSO impacts on Philippine rainfall during the SWM season.

3.4 Numerical Experiment

This study performed a numerical experiment in order to examine the behaviour and mechanism of the potential indicators responsible for the rainfall decline during SWM season in the western part of the Philippines.

3.4.1 Domain Set Up

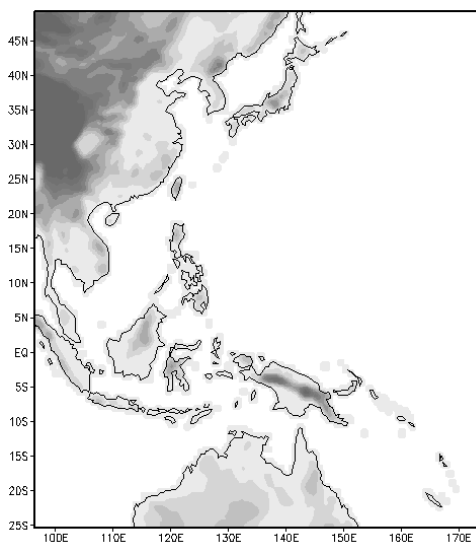


Figure 1: Model Domain Configuration

The Regional Climate model was run using a single domain and has a horizontal resolution of 50 km. The horizontal grid of the model has an Arakawa-Lamb B-staggering of the velocity variables with respect to the scalar variables. The domain cartographic projection is Normal Mercator, which is a suitable projection for the low latitudes located up to 30 degrees and crossing the equator ([Elguindi et al., 2013](#)). The vertical level is set to 18, which is the default of the model. The vertical coordinate is terrain following, which means that the lower grid level follows the terrain but becomes progressively flatter in the upper levels.

$$\sigma = \frac{(p - p_t)}{p_s - p_t} \quad (1)$$

where: σ is a dimensionless coordinate model level, p is the pressure, p_t is a specified constant top pressure and p_s is the surface pressure. Equation 1 shows that at the surface the σ is one.

3.4.2 Data set for the Boundary Conditions

This numerical experiment used ECMWF INTERIM (EIN15) 10-year reanalysis data as initial and boundary conditions. The boundary conditions contain surface temperature, pressure, horizontal three-dimensional wind components, three-dimensional temperature, and mixing ratio. The ECMWF INTERIM has horizontal and vertical resolutions of $1.5^\circ \times 1.5^\circ$ and 37 levels, respectively (see <http://apps.ecmwf.int/datasets/data/interim-full-moda/levtype=sfc/>, last accessed October 2014). Further, the global SST data set used in this experiment was the ERA Interim Project SST, which has 6-hourly temporal and $1.5^\circ \times 1.5^\circ$ horizontal resolutions ([Elguindi et al., 2013](#)) (see <http://apps.ecmwf.int/datasets/data/interim-full-moda/levtype=sfc/>, last accessed October 2014).

3.4.3 Model Configuration

Table 3 shows the summary of the model configuration for the numerical experiment used in this study. The temporal coverage of the numerical simulation is from January 1, 1998 to December 1, 2014. Hence, the spin up time is 6 months at the time of the start of the analysis (June 1, 1998). The convective precipitation scheme over land and ocean that was used in this study is MIT-Emanuel Scheme. MIT-Emanuel scheme was used in other studies to simulate ENSO events (e.g. [Arini et al., 2015](#)). According to [Emanuel \(1991\)](#), and [Emanuel](#)

and Zivkovic-Rothman (1999), this scheme is more advantageous to use because it includes more realistic model for convection and it directly transforms the water into precipitation inside the cumulus clouds. MIT scheme has a parcel precipitation efficiencies that determines the amount of cloud water that converts into precipitation inside the cumulus clouds. However, MIT-Emanuel scheme produced a wet bias over land areas, especially in extreme events (Elguindi et al., 2013).

Table 3. Set Up of Numerical Experiment

Description	
Domain	
cartographic	
projection	Normal Mercator
Grid	point
horizontal	
resolution in km	50
Type of Sea	
Surface	
Temperature used	ERSST
Type of global	
analysis datasets	
used	EIN15
Start date for ICBC	
data generation	1998010100
End data for ICBC	
data generation	2014120100
Global start	1998010100
Start date of this	
run	1998010100
End date for this	
run	2014120100
Cumulus	
convection	
scheme Over Land Emanuel (1991)	
Cumulus	
convection	
scheme	Over
Ocean	Emanuel (1991)
Ocean	Flux
scheme	Zeng et al. (1998)
Planetary	
Boundary	
Condition	Holtslag

Land	Surface
Model	Community Land Model

The Ocean flux parameterization scheme that was used was Zeng. Unlike the BATS scheme, Zeng provides all the stability conditions and gustiness velocity in the model (Elguindi et al., 2013). This Zeng scheme added gustiness velocity so that the induced fluxes were accounted in the boundary layer scale variability and this contributes in the turbulent layer from convective boundary layer to the surface. The following are the bulk aerodynamic algorithms used for computing the sensible heat (SH), latent heat (LH), and momentum fluxes (τ) :

$$\tau = \rho_a u_*^2 (u_x^2 + u_y^2)^{1/2} / u \quad (2)$$

$$SH = -\rho_a C_{pa} u_* \theta_* \quad (3)$$

$$LH = -\rho_a L_e u_* q_* \quad (4)$$

Where u_x and u_y are mean wind components, u_* is the frictional wind velocity, θ_* is the temperature scaling parameter, q_* is the specific humidity scaling parameter, ρ_a is air density, C_{pa} is specific heat of air, and L_e is the latent heat of vaporization (Zeng et al., 1998). According to Francisco et al. (2006), there was an uncertainty in using a specific surface flux scheme, and it depends on the location. For example, the results of the NCEP and BATS, and, ERA40 and Zeng have the same outcome in the study of Francisco et al. (2006).

The land surface model in RegCM was composed of two packages, which are the Biosphere-Atmosphere Transfer Scheme (BATS) and the Community Land Model (CLM). BATS is the default land surface model of RegCM, which is composed of twenty vegetation types. There were modifications in the BATS model for urban and sub-urban developments. In urban development, the modifications were in the runoff and evapotranspiration and not only in the surface albedo that change the energy balance at the surface. The second land surface model is CLM, which is more detailed compared to the first one. There were three modifications in this surface model which are (1) the application of input data in a high resolution, (2) enhancement of the resolution of grids in coast lines, and (3) update of the initialization of soil moisture based on the climatological mean. According to Nayak et al. (2015), BATS performed well during summer in India region compared to CLM. The CLM produce

warmer climate compared to BATS because it produced higher sensible heat flux compared to its latent heat flux, which resulted in a warm bias. However, Wang et al. (2015) stated that CLM performs best in Tibetan Plateau (TP). The reason for this is that CLM has more detailed land surface process that possibly reduced the overestimation of the precipitation in the model. In addition, BATS has higher soil moisture, evapotranspiration, and heating effects in the TP location. In this study, the land surface scheme is CLM and the convective precipitation scheme is MIT-Emanuel. The overall model configuration was based on the results of Juneng et al. (2016), which they performed a sensitivity test of cumulus and air-sea parameterizations using the South East Asian domain.

4. Results

Results have shown that the possible indicators are associated with the changes in SWM rainfall. Numerical simulations can further establish and help under-stand the mechanism of the possible indicators (wind speed, SST, sea level pressure and large scale precipitation) that influence the behavior of rainfall during the SWM season in the past 54 years. Here, the ability of the model to capture the observed patterns of the indicator variables, including during ENSO years, is investigated.

Figure 2 shows the results of the numerical experiment and validation with the observed data. In comparison to the observed data, the model overestimated the precipitation during EN and LN events; and underestimated rainfall in the normal years. However, the general behavior of precipitation during ENSO years were simulated. For example, the EN years showed a positive anomaly and negative anomaly during LN years is not clearly simulated.

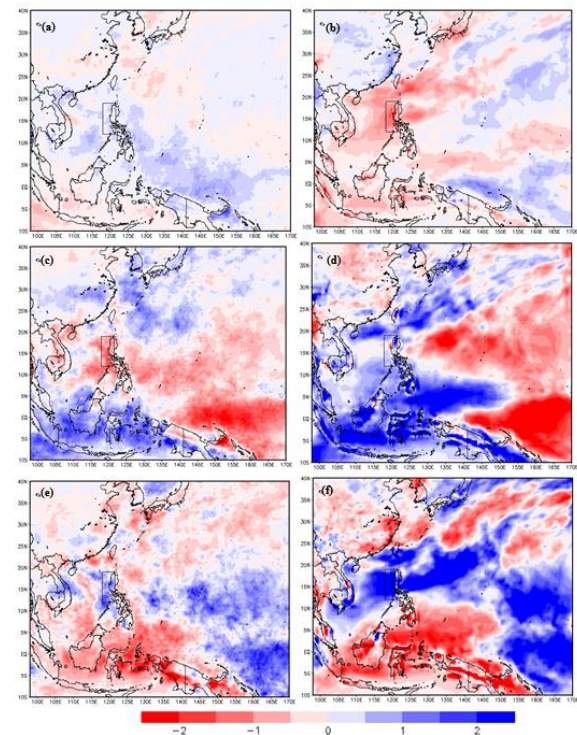


Figure 2. Precipitation Anomaly from 1998 to 2014 for (a) Normal Years, (c) LN, and (e) EN of TRMM. Results of RegCM using CLM during (b) Normal years, (d) LN and (f) EN. (units: mm/day)

Figures 3a, 3c and 3e show the observed data from NOI – SST and the model results are shown in Figures 3b, 3d and 3f. SST was well simulated by the model. Figure 3 also shows the reversal of the ENSO events during SWM season. EN (LN) years show the negative (positive) anomaly in the west Philippine Sea.

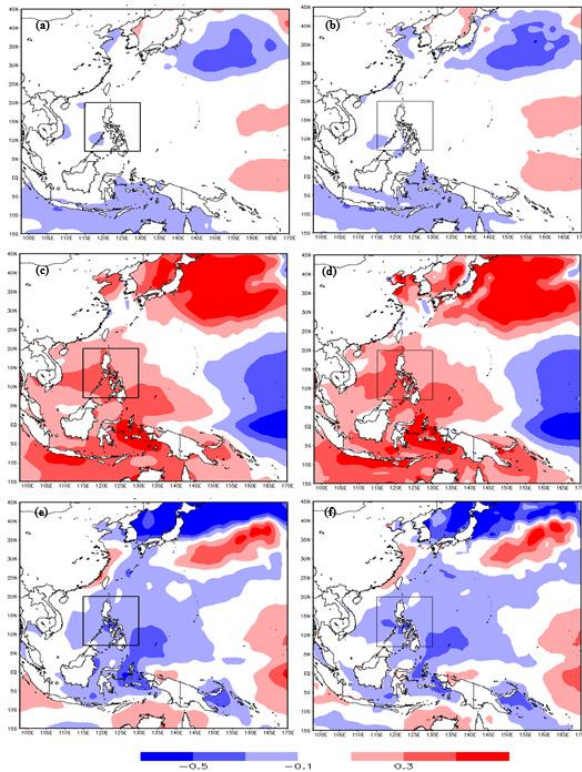


Figure 3. SST Anomaly from 1998 to 2014 for (a) Normal Years, (c) LN, and (e) EN of NOI-SST. Results of RegCM using CLM during (b) Normal years, (d) LN and (f) EN. (units: degrees Celsius)

Figures 4a to 4f show the simulated results and observed data for sea level pressure. Similar to the results for SST, the model was able to capture the behavior of sea level pressure during ENSO years. The opposite behavior during EN and LN were well simulated especially in the Western Pacific. The EN has a negative anomaly of sea level pressure located at the Western Pacific and positive anomaly during LN events. However, the model overestimated the sea level pressure at the northwestern part of the country during LN and underestimated during EN. The results of the model, however, are very close to the observed data. Dash et al. (2013) have also shown that RegCM4 captures the behavior of mean sea level pressure of NCEP-NCAR.

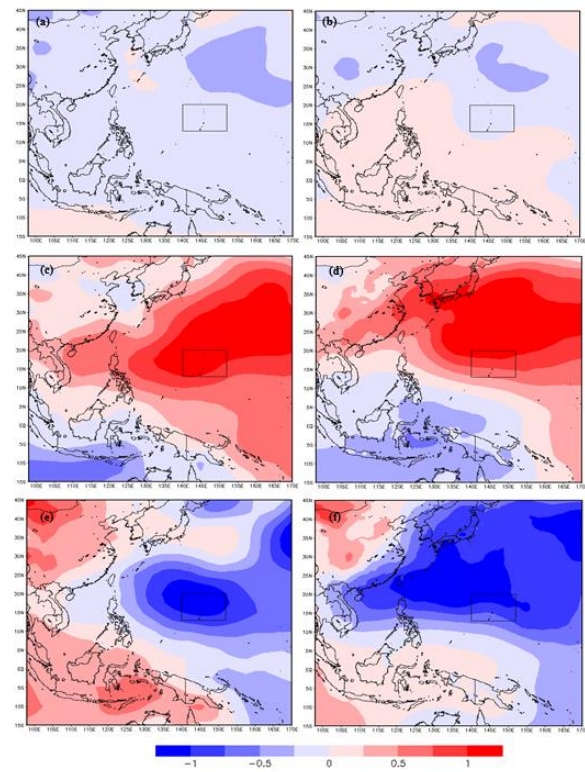


Figure 4. Pressure Anomaly from 1998 to 2014 for (a) Normal Years, (c) LN, and (e) EN of NCEP-NCAR. Results of RegCM using CLM during (b) Normal years, (d) LN and (f) EN. (units: hPa)

Figure 5 shows the comparison between the observed data and the model results for wind anomaly. Results show that the model does not capture the behavior of the wind anomaly. There was an underestimation at the Indo Pacific region during Normal Years. In addition to this, there was an overestimation of winds at the Eastern Part of the Philippines during LN events. Only during El Niño events is the model approximately closer to the observed data. The inability of the model to simulate winds and wind patterns accurately can be the reason why it is not able to capture the behavior of precipitation. For example the result of the model for Normal years has a drier condition compare to normal because if we look at the result of the wind anomaly for Normal years, there is a decrease of wind speed simulated during normal years. Wu et. al (2009) and Peralta and Narisma (2014) have also shown that there is a direct positive relationship between wind speed and rainfall. Wu et al. 2009 states that: "During the ENSO-developing (decaying) summer, the rainfall–SST correlation is significantly positive (negative).

The former leads to negative rainfall anomalies in the western Pacific, whereas the latter leads to a cold SST anomaly resulting from enhanced surface latent heat fluxes. The negative correlation is attributed to the maintenance of an anomalous Philippine Sea anticyclone from the El Niño peak winter to the subsequent summer. The anomalous anticyclone, on one hand, suppresses the local rainfall, and on the other hand induces a warm in situ SST anomaly through both the enhanced solar radiation (resulting from a decrease in clouds) and the reduced surface latent heat flux (resulting from the decrease of the monsoon westerly).

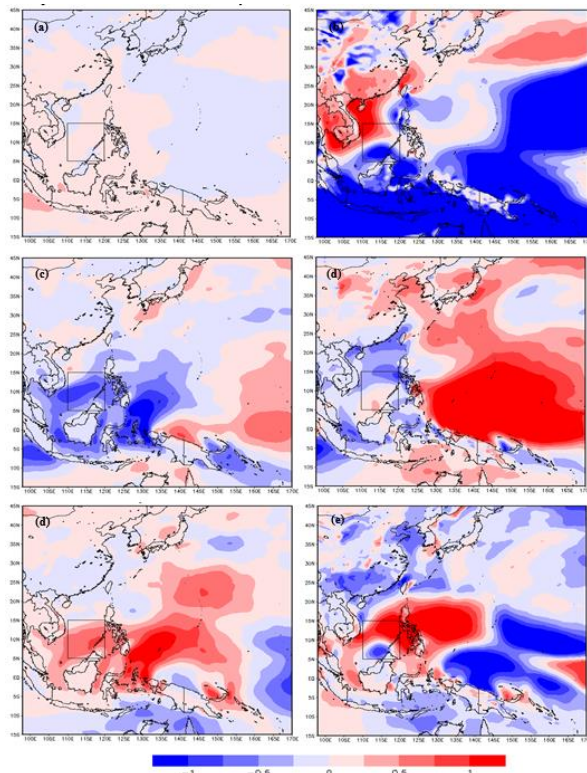


Figure 5. Wind Anomaly from 1998 to 2014 for (a) Normal Years, (c) LN, and (e) EN of ERA-Interim. Results of RegCM using CLM during (b) Normal years, (d) LN and (f) EN. (units: m/s)

In summary, the model results almost capture the behaviour and patterns of the observed variable indicators during ENSO years. During El Niño the model shows an increase in precipitation in the SWM affected regions and a decrease in sea level pressure in the Northeast Pacific. SST is also cooler in the west Philippine Sea. During La Niña, precipitation is lower than normal. SST and sea level pressure are higher than normal, exhibiting an opposite behaviour during El Niño. The model

partly confirms that the variable indicators (of SST, sea level pressure and wind) affects precipitation in the western regions of the Philippines during SWM season.

5. Discussion

Most of the results of numerical experiment captured the behavior and patterns of the observed data. For example, the anomaly of precipitation of EN event is captured well by the model. However, some results are not captured well by the model. For example, the model has a negative anomaly in the western part of the country during normal years. The behavior of the wind anomalies are also not captured by the model. This is one of the reasons why the model fails to capture the rainfall patterns during ENSO events. Model results, however, are consistent with the behavior of the possible indicators of SST and sea level pressure during the ENSO signal reversal of ENSO events. The configuration of the model has a good set up to capture the SST and sea level pressure. In conclusion, the results of the study show that SST, wind and pressure are indicators for and are associated with rainfall behavior in the western parts of the country during the SWM season. The recommendation of the researcher is to investigate other components of the model like the cumulus parameterization schemes or land cover change.

References

- [1] Arini, E. Y., Hidayat, R., & Faqih, A. (2015). Rainfall Simulation Using RegCM4 Model in Kalimantan during El Nino Southern Oscillation. *Procedia Environmental Sciences*, 24, 70-86.
- [2] Asuncion, J. F., & Jose, A. M. (1980). A study of the characteristics of the northeast and southwest monsoons in the Philippines. *NRCP Assisted Project*, 49.
- [3] Cruz, F. T., Narisma, G. T., Villafuerte, M. Q., Chua, K. C., & Olaguera, L. M. (2013). A climatological analysis of the southwest monsoon rainfall in the Philippines. *Atmospheric Research*, 122, 609-616.
- [4] Dash, S. K., Mamgain, A., Pattnayak, K. C., & Giorgi, F. (2013). Spatial and temporal variations in Indian summer monsoon rainfall and temperature: an analysis based on

- RegCM3 simulations. *Pure and Applied Geophysics*, 170(4), 655-674.
- [5] De las Alas, J. G., & Buan, R. D. (1986). Preliminary study on the effects of El Nino on rainfall at selected Philippine regions. *Natural and Applied Science Bulletin (Philippines)*.
- [6] Elguindi, N., Bi, X., Giorgi, F., Nagarajan, B., Pal, J., Solmon, F., ... & Giuliani, G. (2011). Regional climatic model RegCM user manual version 4.1. ITC, Trieste, Italy.
- [7] Emanuel, K. A. (1991). A scheme for representing cumulus convection in large-scale models. *Journal of the Atmospheric Sciences*, 48(21), 2313-2329.
- [8] Emanuel, K. A., & Živkovic-Rothman, M. (1999). Development and evaluation of a convection scheme for use in climate models. *Journal of the Atmospheric Sciences*, 56(11), 1766-1782.
- [9] Franchito, S. H., Rao, V. B., Vasques, A. C., Santo, C. M., & Conforte, J. C. (2009). Validation of TRMM precipitation radar monthly rainfall estimates over Brazil. *Journal of Geophysical Research: Atmospheres*, 114(D2).
- [10] Francisco, R. V., Argete, J., Giorgi, F., Pal, J., Bi, X., & Gutowski, W. J. (2006). Regional model simulation of summer rainfall over the Philippines: Effect of choice of driving fields and ocean flux schemes. *Theoretical and applied climatology*, 86(1-4), 215-227.
- [11] Flores, J.F., Balagot, V.F., 1969. *Climate of the Philippines*. World survey of climatology, vol. 8. Elsevier Scientific Publishing Company, Amsterdam, pp. 159–213.
- [12] Jose, A. M., Francisco, R. V., & Cruz, N. A. (1996). A study on impact of climate variability/change on water resources in the Philippines. *Chemosphere*, 33(9), 1687-1704.
- [13] Juneng, L., F. Tangang, J.X. Chung, S.T. Ngai, T.W. Teh, G. Narisma, F. Cruz, T. Phan-Van, T. Ngo-Duc, J. Santisirisomboon, P. Singhruck, D. Gunawan and E. Aldrian, 2016. Sensitivity of the Southeast Asia Rainfall Simulations to Cumulus and Air-Sea Flux Parameterizations in RegCM4. *Climate Research*, doi:10.3354/cr01386
- [14] Kao, H. Y., & Yu, J. Y. (2009). Contrasting eastern-Pacific and central-Pacific types of ENSO. *Journal of Climate*, 22(3), 615-632.
- [15] Lang, S., Tao, W. K., Simpson, J., Cifelli, R., Rutledge, S., Olson, W., & Halverson, J. (2007). Improving simulations of convective systems from TRMM LBA: Easterly and westerly regimes. *Journal of the atmospheric sciences*, 64(4), 1141-1164.
- [16] Lyon, B., & Camargo, S. J. (2009). The seasonally-varying influence of ENSO on rainfall and tropical cyclone activity in the Philippines. *Climate dynamics*, 32(1), 125-141.
- [17] Lyon, B., Cristi, H., Verceles, E. R., Hilario, F. D., & Abastillas, R. (2006). Seasonal reversal of the ENSO rainfall signal in the Philippines. *Geophysical research letters*, 33(24).
- [18] Meehl, G. A. (1994). Influence of the land surface in the Asian summer monsoon: External conditions versus internal feedbacks. *Journal of climate*, 7(7), 1033-1049.
- [19] Moya, T. B., & Malayang Iii, B. S. (2004). Climate variability and deforestation-reforestation dynamics in the Philippines. In *Tropical Agriculture in Transition—Opportunities for Mitigating Greenhouse Gas Emissions?* (pp. 261-277). Springer Netherlands.
- [20] Nayak, S., Mandal, M., & Maity, S. (2015). Customization of regional climate model (RegCM4) over Indian region. *Theoretical and Applied Climatology*, 1-16.
- [21] Peralta, J.C., Narisma, G.T., The Influence of Warmer Sea Surface Temperatures in the South China Sea on Southwest Monsoon Rainfall in the Philippines, 2014.
- [22] Roxy, M., Tanimoto, Y., Preethi, B., Terray, P., & Krishnan, R. (2013). Intraseasonal SST-precipitation relationship and its spatial variability over the tropical summer monsoon region. *Climate dynamics*, 41(1), 45-61.
- [23] Roy, I., & Haigh, J. D. (2010). Solar cycle signals in sea level pressure and sea surface temperature. *Atmospheric Chemistry and Physics*, 10(6), 3147-3153.
- [24] Stock, C. A., Pegion, K., Vecchi, G. A., Alexander, M. A., Tommasi, D., Bond, N. A., et al. (2015). Seasonal sea surface temperature anomaly prediction for coastal ecosystems.

- Progress in Oceanography, 137, 219–236.
<https://doi.org/10.1016/j.pocean.2015.06.007>
- [25] Trenberth, K. E. (1997). The definition of el nino. *Bulletin of the American Meteorological Society*, 78(12), 2771-2777.
- [26] Wang, X., Yang, M., & Pang, G. (2015). Influences of Two Land-Surface Schemes on RegCM4 Precipitation Simulations over the Tibetan Plateau. *Advances in Meteorology*, 2015.
- [27] Wu, B., Li, T., & Zhou, T. (2010). Asymmetry of atmospheric circulation anomalies over the Western North Pacific between El Niño and La Niña*. *Journal of Climate*, 23(18), 4807-4822.
- [28] Wu, B., Zhou, T., & Li, T. (2009). Contrast of Rainfall-SST Relationships in the Western North Pacific between the ENSO-Developing and ENSO-Decaying Summers*. *Journal of climate*, 22(16), 4398-4405.
- [29] Xie, S. P., Deser, C., Vecchi, G. A., Ma, J., Teng, H., & Wittenberg, A. T. (2010). Global warming pattern formation: sea surface temperature and rainfall*. *Journal of Climate*, 23(4), 966-986.
- [30] Yu, J. Y., & Kim, S. T. (2011). Relationships between extratropical sea level pressure variations and the central Pacific and eastern Pacific types of ENSO. *Journal of Climate*, 24(3), 708-720.
- [31] Zeng, X., Zhao, M., & Dickinson, R. E. (1998). Intercomparison of bulk aerodynamic algorithms for the computation of sea surface fluxes using TOGA COARE and TAO data. *Journal of Climate*, 11(10), 2628-2644.